MECHANICAL AND ELECTRICAL PROPERTIES OF TERNARY CU-NI-ZN ALLOYS

Milena Premović[33]; Milan Kolarević[34]; Aleksandar Đorđević[35]; Tao Xiaoma[36]; Pavel Brož[37]

Abstract

Selected ternary system is chosen due to the significant interest of nickel alloys in the different industry such as electronic, chemical, automotive, marine etc. Chosen ternary system up to this paper has not been studied. In this paper mechanical and electrical properties were measured. By using experimentally determined value for electrical conductivity and hardness a mathematical model for both properties were develop. Presented mathematical model was used for calculation of electrical properties and hardness along all composition ranges.

Key words: *Hardness, electrical properties, isothermal section at 25 °C*

Introduction

Nickel and nickel-based alloys are widely used in different industries [1-4], such as electronic, chemical, automotive, marine etc. Alloys are used for making vessels, pipes, heat exchangers, pumps, impellers, valves [5], alkaline batteries, gas engines and turbines [6], optical mirrors [7, 8], equipment for food industry, chemical industry, petrochemical industry, as well as for galvanic coating of steel objects and other type of equipment. Due to the significant applications of alloys it is highly necessary to study Ni-based alloys. Up to now a lot of binary alloys were studied but typically applicable alloys consist of more elements, it is therefore necessary to study systems which consist of three, four and more elements. Ternary systems based on Bi-Ni [9-12] were studied in past but still some of the ternaries were not tested. Chosen system in our study is Bi-Ni-Zn since there is no study related to it. The

[33]Milena Premović, PhD, Assistant professor, Academician of IRASA, State Key Laboratory of Powder Metallurgy, Central South University, Changsha, Hunan PR China; University of Priština, Faculty of Technical Science, Kos. Mitrovica, Republic of Serbia, milena.premovic@gmail.com
[34]Milan Kolarević, PhD, Faculty of Mechanical Engineering, University of Kragujevac, Kraljevo, Republic of Serbia, kolarmi@mts.rs
[35]Aleksandar Đorđević, MA, Teaching assistant, University of Priština, Faculty of Technical Science, Kos. Mitrovica, Republic of Serbia, aleksandar.djordjevic@pr.ac.rs
[36]Tao Xiaoma, PhD, Full professor, Academician of IRASA, Guangxi University, Nanning, PR China, taoxiaoma@gxu.edu.cn
[37]Pavel Brož, PhD, Associate professor, Academician of IRASA, Masaryk University, Faculty of Science, Department of Chemistry, Brno, Czech Republic, broz@chemi.muni.cz

focus of this study is on experimental investigation of phase equilibria in a ternary Bi-Ni-Zn system. The ternary Bi-Ni-Zn system has not been experimentally investigated before.

In the present study, three series of the samples prepared for experimental investigation. The as-cast samples from three vertical sections were investigated using differential thermal analysis (DTA). The samples annealed at 400 and 700 °C were studied by means of scanning electron microscopy (SEM) together with energy dispersive spectrometry (EDS) and X-ray diffraction analysis (XRD) with samples in a powder form.

In parallel with that, phase diagrams of the investigated ternary system Bi-Ni-Zn were calculated by using thermodynamic parameters for the constitutive binary systems reported in literature [13-17]. The calculated results that include phase diagrams of the experimentally investigated sections, liquidus projection and invariant reactions were compared with the obtained experimental results and a close mutual agreement was observed.

Thermodynamic calculation

Calculated phase diagram of constitutive binary systems for ternary Bi-Ni-Zn system are shown in Fig. 1. Optimized thermodynamic parameters for those binaries are taken from literature [13–17].

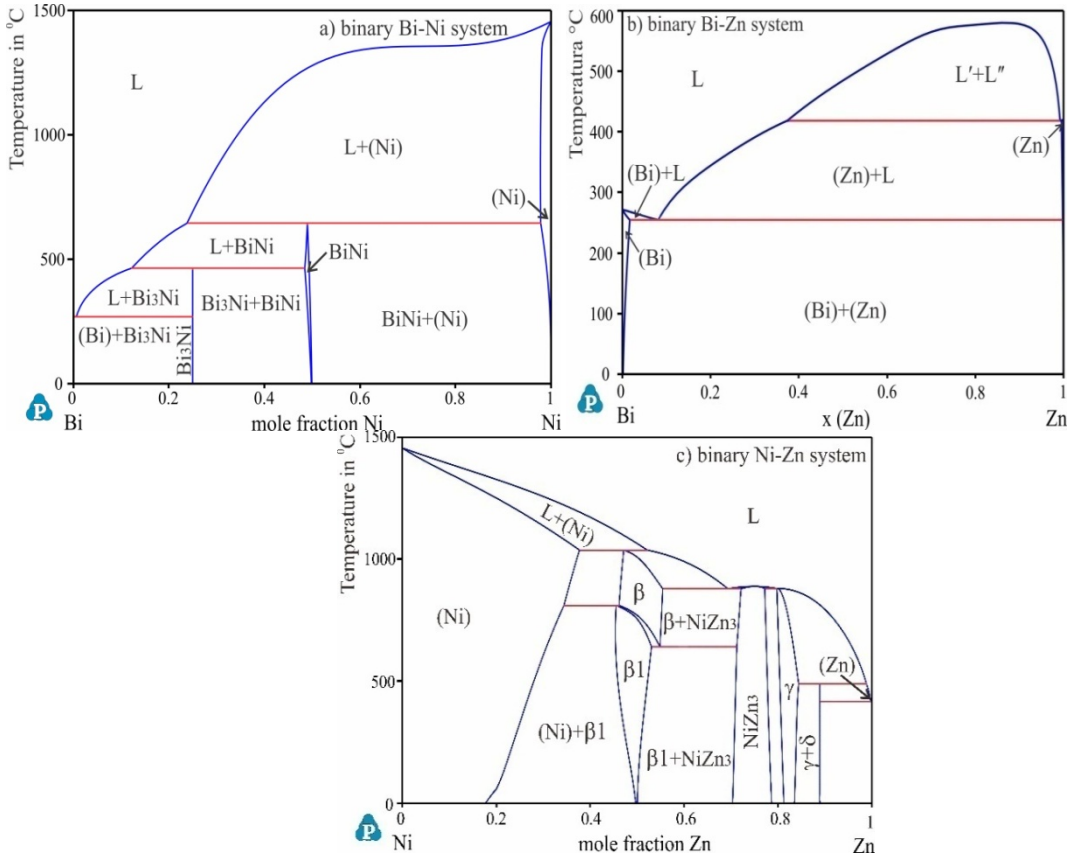

Figure 1: Calculated binary phase diagrams a) Bi-Ni system [13-15], b) Bi-Zn system [16], and c) Ni-Zn system [17].

Based on the literature information for binary sub-systems crystallographic data for phases in the ternary Bi-Ni-Zn system are summarized and presented in Table 1 [18-27].

Table 1: Considered phase, their crystallographic data and database names for the phases of the ternary Bi-Ni-Zn systems

Phase	Pearson symbol	Space group	Lattice parameters (Å)			Ref.
			a	*b*	*c*	
Liquid	-	-				
(Bi)	*hR*2	$R\bar{3}m$	4.535(2)		11.814(6)	[18]
(Ni)	*cF*4	$Fm\bar{3}m$	3.5243			[19]
(Zn)	*hP*2	$P6_3/mmc$	2.665		4.947	[20]
Bi_3Ni	*oP*16	*Pnma*	8.879	4.0998	11.483	[21]
BiNi	*mC*64	$F12/m1$	14.124	8.1621	21.429	[22]
β	*cP*2	$Pm\bar{3}m$	2.908			[23]
β1	*tP*2	$P4/mmm$	2.747		3.190	[24]
γ	*cI*52	$I\bar{4}3m$	8.941			[24,25]
δ	*mC*50	C_{12}/m_1	13.37	7.47	7.65	[26]
$NiZn_3$	*oA*276	*Abm*2	33.326	8.869	12.499	[27]

Experimental procedure

The ternary samples were prepared by using high purity (99.999atomic%) elements Bi, Ni and Zn produced by Alfa Aesar (Germany). Samples were measured in different molar ration and the total masses of the ternary alloy samples were about 3 g. Weighed masses of the pure metals were arc-melted under a high purity argon atmosphere using a non-consumable tungsten electrode. Obtained samples were re-melted six times in order to improve homogeneity and then slowly cooling to room temperature. The average weight loss of the samples during melting was about 0.5 %of the total weight.

Such prepared samples were divided into three groups. Samples from first and second group were subjected to the SEM-EDS test. Samples from third group for DTA tests. All samples from 1st and 2nd group were firstly tested by XRD. Device for XRD test was D2 PHASER, Bruker, Germany powder diffractometer equipped with a dynamic scintillation detector and ceramic x-ray Cu tube (KFL-Cu-2 K).

Samples from 1st and 2nd group were put into quartz glass ampoules, sealed under vacuum and annealed at 400 and 700 °C temperatures for six weeks, respectively. After annealing samples were quenched into ice water in order to preserve the equilibrium compositions. Those samples were subjected to the SEM-EDS and XRD test. Used device for SEM-EDS analysis was JEOL JSM-6460 scanning electron microscope with energy dispersive spectroscopy (EDS) (Oxford Instruments X-act).

Samples from last group were used for phase transition temperature determination which were measured by DTA method. The DTA measurements were performed on a DTG-60H (Shimadzu). Alumina crucibles were used and measurements were performed under flowing argon atmosphere. Samples weighing between 20 and 30 mg were investigated at a heating rate of 5 °C/min with three cycles of heating and

cooling. The sample masses and heating rates were determined by analysis of one sample at different testing conditions. The reference material was empty alumina crucible. The overall uncertainty of the determined phase transformation temperatures was estimated to be ±1 °C.

Results and discussion

Six ternary samples annealed at 400 °C were analyzed using SEM–EDS and XRD method. Results of test are summarized in Table 2

Table 2: EDS and XRD results of the ternary Bi-Ni-Zn samples annealed at 400 °C for six weeks

N.	Composition of samples x(at. %)	Determined phases		Compositions of phases x(at.%)		
		EDS	XRD	Bi	Ni	Zn
1	16.33Bi 73.95 Ni 9.72 Zn	(Ni) BiNi	(Ni) BiNi	1.51±0.01 50.29±0.03	82.65±0.01 49.23±0.02	15.84±0.05 0.48±0.04
2	17.11 Bi 58.84 Ni 24.05 Zn	(Ni) BiNi β1	(Ni) BiNi β1	1.93±0.01 50.30±0.02 0.28±0.07	72.2±0.03 48.67±0.04 53.04±0.05	25.87±0.01 1.03±0.01 46.68±0.02
3	34.04 Bi 44.26 Ni 21.70 Zn	Bi3Ni BiNi β1	Bi3Ni BiNi β1	74.59±0.05 49.41±0.03 0.69±0.01	24.55±0.05 49.70±0.07 51.73±0.02	0.86±0.05 0.89±0.06 47.58±0.07
4	28.06 Bi 27.54 Ni 44.40 Zn	NiZn3 L β1	NiZn3 - β1	0.28±0.07 94.34±0.04 0.69±0.03	27.97±0.01 2.51±0.01 48.41±0.05	71.75±0.01 3.15±0.02 50.90±0.03
5	48.24 Bi 20.02 Ni 31.74 Zn	NiZn3 L β1	NiZn3 - β1	1.51±0.07 94.34±0.05 0.71±0.01	28.1±0.03 3.25±0.08 46.91±0.02	70.39±0.05 2.41±0.06 52.38±0.04
6	23.54 Bi 3.26 Ni 73.20 Zn	L (Zn) δ	- (Zn) δ	64.50±0.02 1.31±0.04 0.89±0.05	0.46±0.01 0.73±0.03 9.79±0.03	35.04±0.03 97.96±0.05 89.32±0.08

By using the EDS analyzer, the compositions of the samples and the compositions of the observed phases were determined.
For the purpose of determining a phase equilibria at 700 °C, seven ternary alloy samples were prepared and tested by SEM-EDS and XRD. The results of the SEM–EDS and XRD are summarized in Table 3.

Table 3: EDS and XRD results of the ternary Bi-Ni-Zn samples annealed at 700 °C for six weeks

N.	Composition of samples x(at. %)	Determined phases		Compositions of phases x(at. %)		
		EDS	XRD	Bi	Ni	Zn
1	21.68 Bi 71.27 Ni 7.05 Zn	(Ni) L	(Ni) -	3.36±0.07 80.77±0.01	88.00±0.02 18.32±0.01	8.64±0.04 0.91±0.03
2	31.15 Bi 51.25 Ni 17.60 Zn	(Ni) L	(Ni) -	1.13±0.02 81.38±0.05	71.58±0.05 16.91±0.07	27.29±0.05 1.71±0.07
3	41.86 Bi 37.77 Ni 20.37 Zn	(Ni) L β1	(Ni) - β1	0.48±0.04 82.21±0.02 0.48±0.03	66.95±0.03 15.57±0.08 53.13±0.01	32.57±0.06 2.22±0.03 46.39±0.01
4	43.01 Bi 30.06 Ni 26.93 Zn	L β1	- β1	82.21±0.07 1.31±0.01	11.33±0.05 50.31±0.02	6.46±0.07 48.38±0.05

N.	Composition of samples x(at. %)	Determined phases		Compositions of phases x(at. %)		
		EDS	XRD	Bi	Ni	Zn
5	36.07 Bi 23.73 Ni 40.20 Zn	L NiZn3 β	- NiZn3 β	83.03±0.05 0.71±0.02 0.69±0.08	5.58±0.01 29.22±0.07 43.43±0.04	11.39±0.02 70.07±0.08 55.88±0.03
6	22.71 Bi 19.34 Ni 57.95 Zn	L NiZn3	- NiZn3	82.61±0.02 0.87±0.01	2.48±0.03 24.74±0.02	14.91±0.01 74.39±0.04
7	21.89 Bi 12.93 Ni 65.18 Zn	L γ	- γ	65.53±0.03 0.92±0.04	1.25±0.01 18.61±0.07	33.22±0.03 80.47±0.07

Twelve ternary samples from three different vertical section were used for DTA tests. Composition of tested samples were checked with EDS method. Summary of DTA and EDS results are presented in Table 4.

Table 4: Phase transition temperatures of the studied alloys from the ternary Bi-Ni-Zn system determined by DTA at pressure p=0.1 MPa.

Composition (at.%)		Temperatures of phase transformation (°C)*		
nominal	EDS	Ternary reactions	monovariant	Liquidus
Vertical section Bi–$Ni_{50}Zn_{50}$				
$Bi_{20}Ni_{40}Zn_{40}$	$Bi_{20.11}Ni_{39.80}Zn_{40.09}$	268.3	342.8/753.8	953.1
$Bi_{40}Ni_{30}Zn_{30}$	$Bi_{38.78}Ni_{30.18}Zn_{31.04}$	274.8	322.1/726.1	943.8
$Bi_{60}Ni_{20}Zn_{20}$	$Bi_{61.07}Ni_{20.56}Zn_{18.37}$	271.8	722.1	907.3
$Bi_{80}Ni_{10}Zn_{10}$	$Bi_{79.52}Ni_{10.03}Zn_{10.45}$	273.1	711.9	
Vertical section Ni–$Bi_{50}Zn_{50}$				
$Bi_{40}Ni_{20}Zn_{40}$	$Bi_{40.89}Ni_{20.71}Zn_{38.40}$	260.1/647.3/851.9		919.7
$Bi_{30}Ni_{40}Zn_{30}$	$Bi_{29.76}Ni_{39.61}Zn_{30.63}$	265.1/463.1/806.3	970.8	
$Bi_{20}Ni_{60}Zn_{20}$	$Bi_{19.18}Ni_{59.73}Zn_{21.09}$	498.3		1218.3
$Bi_{10}Ni_{80}Zn_{10}$	$Bi_{9.13}Ni_{79.15}Zn_{11.72}$		591.8	1315.7
Vertical section Zn–$Bi_{50}Ni_{50}$				
$Bi_{40}Ni_{40}Zn_{20}$	$Bi_{41.08}Ni_{39.81}Zn_{19.11}$	453.1/485.7/794.1		1054.3
$Bi_{30}Ni_{30}Zn_{40}$	$Bi_{29.17}Ni_{29.48}Zn_{41.35}$	275.7/647.3	836.4	947.1
$Bi_{20}Ni_{20}Zn_{60}$	$Bi_{19.81}Ni_{20.52}Zn_{59.67}$	277.4		863.1
$Bi_{10}Ni_{10}Zn_{80}$	$Bi_{11.01}Ni_{9.13}Zn_{79.86}$	249.1/493.3		812.4

*temperatures in table are organized by consulting calculated vertical sections

By appearance of peaks on DTA curve temperatures of phase transformation are organized in table 4 as a ternary reaction, monovariant and Liquidus.
Experimentally obtained results presented in previous part are compared with calculated phase diagrams. Calculation of phase diagrams were performed by using Pandat software and thermodynamic dataset constructed based on binary constitutive systems. Constructed thermodynamic dataset is based on literature information from references [13-17].
EDS results given in Tables 2 and 3 are compared with calculated isothermal sections at 400 and 700 °C. Figure 2 presents comparison of the calculated isothermal section at 400 °C and the EDS resultsin Table 2. The obtained experimental results are marked with the same symbol but in different color. Different color is used in order to make a distinction between the EDS composition of different samples.

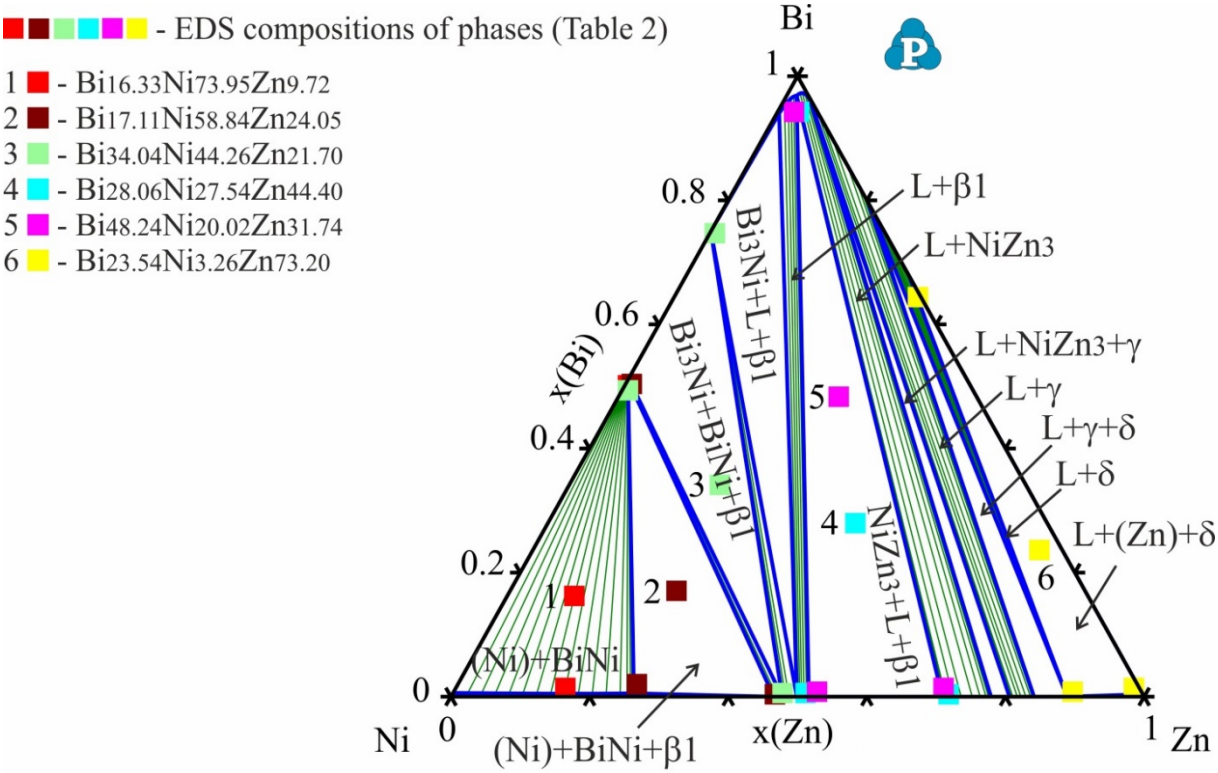

Figure 2: Calculated isothermal section at 400 °C compared with EDS results given in Table 2.

Calculated isothermal section consists of 16 different phase regions. From those 16 regions two are single phase region, L and (Ni) phase regions, seven are two-phase regions and seven three-phase regions. From 16 predicted phase regions five are experimentally confirmed, four three-phase regions and one two-phase region. Composition of sample 1 is located in the (Ni)+BiNi two-phase region, sample 2 in (Ni)+BiNi+β1 three-phase region, sample 3 in Bi3Ni+BiNi+β1 three-phase region, sample 4 and 5 in NiZn3+L+β1 three-phase region and sample 6 in L+(Zn)+δ three-phase region. By comparing compositions of the detected phases for sample 1 to 6 determined by EDS and the related calculated phase compositions it can be noticed that they are in a fairly close agreement.In generall it can be also said that a close overall agreement between the results of calculations and the experiments was obtained.

The EDS results given in Table 3 are compared with the calculated isothermal section at 700 °C. Figure 3, presents comparison of the calculated phase diagram and the EDS results.

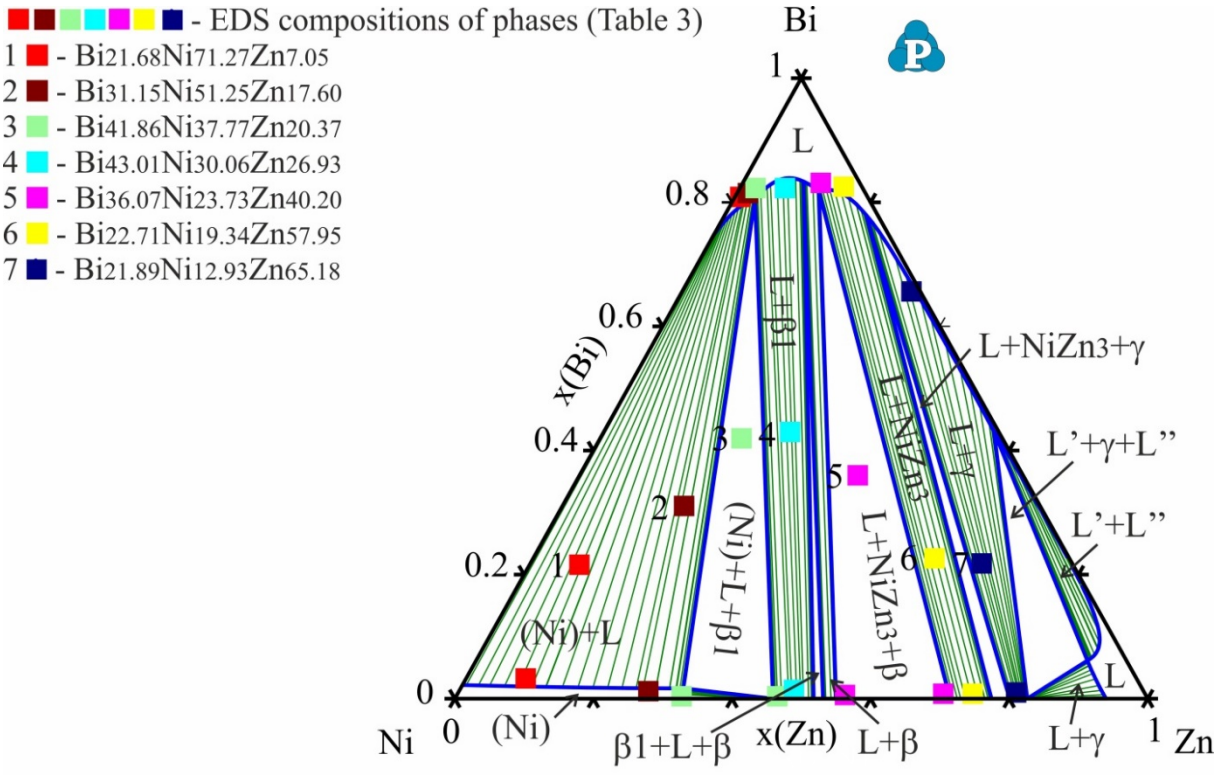

Figure 3: Calculated isothermal section at 700 °C compared with EDS results given in Table 3.

Calculated isothermal section at 700 °C, consists of sixteen phase regions. Calculated phase regions are: three single phase regions, L rich with bismuth, L phase rich with zinc and (Ni) solid solution, eight two phase regions ((Ni)+L, (Ni)+β1, L+β1, L+β, L+NiZn3, L+γ, L'+L" and L+γ) and five three-phase regions ((Ni)+L+β1, β1+L+β, L+NiZn3+β, L+NiZn3+γ and L'+γ+L"). Six of sixteen calculated phase regions are experimentally confirmed. From which four are two-phase regions (Ni)+L (samples 1 and 2), L+β1(sample 4), L+NiZn3 (sample 6) and L+γ (sample 7) and two are three phase regions (Ni)+L+β1(samples 3) and L+NiZn3+β (sample 5) were experimentally verified. Comparison of EDS results given in Table 3 and calculated isothermal section at 700 °C show a very good overall agreement. Experimentally determined composition of phases agree well with calculated composition of phases. In general for both isothermal studies EDS experimental results did not detected significant solubility than is expected and also ternary compounds are not detected.
As a next step, temperature of phase transformations summarized in Table 4 are compared with calculated vertical sectiions and presented in Figure 9.

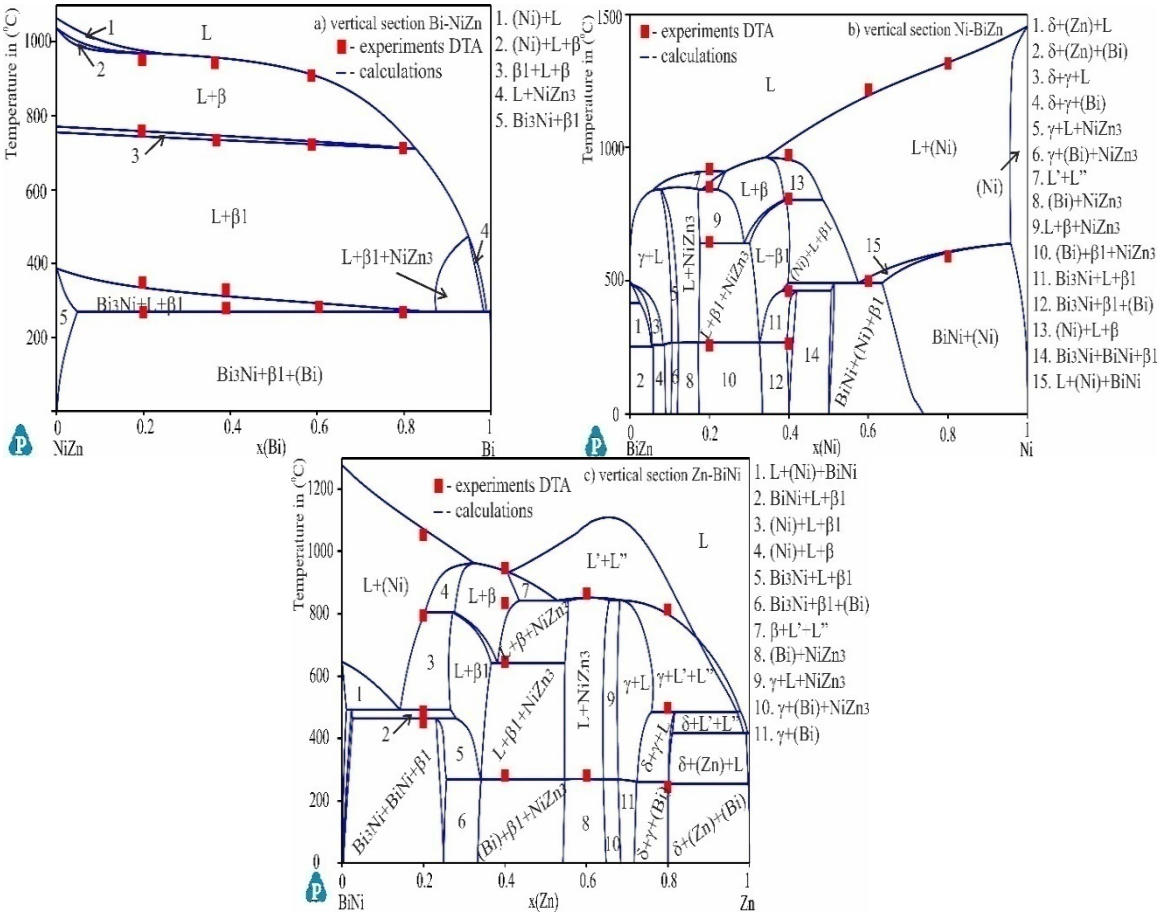

Figure 4: Calculated vertical sections of the ternary Bi-Ni-Zn system compared with DTA experimental results: a) Bi-NiZn, b) Ni-BiZn and c) Zn-BiNi.

As can be seen in Figure 4, good overall agreement between the calculated vertical sections and the DTA results was achieved. By comparing the calculated and the experimentally determined temperatures, it is clear that the highest detected temperatures correspond to the liquidus temperatures.

In general, it can be said that the experimentally determined temperatures of phase transformations support the results of the calculations quite well.

Based on the presented results, it can be safely assumed that it is not necessary to introduce new parameters to describe the ternary Bi-Ni-Zn system. Therefore, the applied thermodynamic dataset was further used for the calculation of a liquidus projection and invariant reactions.

Figure 5, presents prediction of liquidus projection of the ternary Bi-Ni-Zn system, with magnified bismuth and zinc rich part.

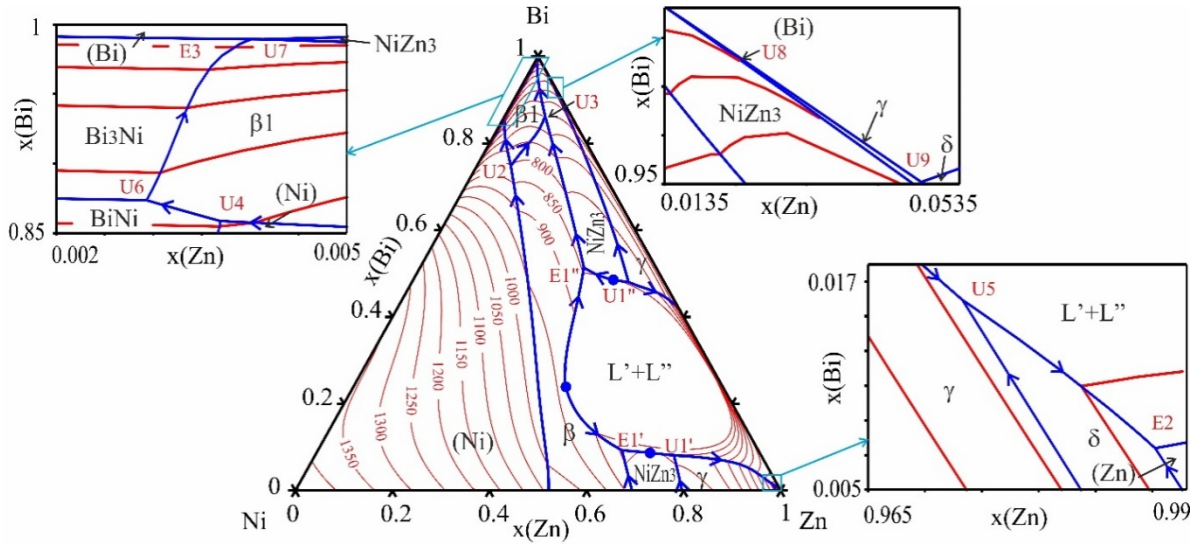

Figure 5:Prediction of liquidus projection of the ternary Bi-Ni-Zn system with magnified Bi and Zn rich part.

Predicted liquidus projection has ten fields of primary crystallization and field of miscibility gap. Twelve invariant reactions were predicted and details are given in Table 5.

Table 5. Predicted invariant reaction of the ternary Bi-Ni-Zn system.

T (°C) Reactions	Type*	Composition of reaction in mole fraction		
		Bi	Ni	Zn
843.49 L′+NiZn3→L″+γ	U1	0.080793	0.179583	0.739624
842.38 L′→L″+NiZn3+β	E1	0.092703	0.280723	0.626574
804.50 β+(Ni)→L+β1	U2	0.747760	0.182174	0.070066
641.38 L+β→NiZn3+β1	U3	0.864691	0.053503	0.081806
492.29 L+(Ni)→β1+BiNi	U4	0.858813	0.137497	0.003690
485.22 L′+γ→L″+δ	U5	0.015942	0.010758	0.973300
464.06 L+BiNi→β1+Bi3Ni	U6	0.873735	0.123334	0.002931
416.93 L′→(Zn)+L″+δ	E2	0.007396	0.002386	0.990219
269.09 L+NiZn3→β1+(Bi)	U7	0.989336	0.006521	0.004143
269.06 L→β1+Bi3Ni+(Bi)	E3	0.989255	0.006738	0.004007
268.53 L+ NiZn3→(Bi)+γ	U8	0.986164	0.000147	0.013689
260.72 (Bi)+γ→L+δ	U9	0.950883	8.064510E-008	0.049117

*U-univariant reaction, E-eutectic reaction, number from 1 to 9 depend on temperature decrease.

Three reactions are E-type (eutectic) and nine are U-type (univariant) reactions. E1 reaction L′→L″+NiZn3+β and E2 reaction L′→(Zn)+L″+δ are monotectic reaction, while E3 reaction L→β1+Bi3Ni+(Bi) is ternary eutectic reaction. U2 and U9 reactions are solid transition reactions, and all others are liquid transition reactions. Eight of twelve predicted invariant reactions are experimenatly confirmed.

Conclusion

Alloys from ternary Bi-Ni-Zn system are experimentally and analiticaly tested for the first time. Experimental results of DTA test were compared with calculated vertical sections. By DTA test temperature of eight invariant reactions have been determined, temperatures of other phase transformation and liquidus temperature. Comparison of DTA results and calculated vertical section shows good agrement betweene calculated and experimentally determined temperatures of phase transformation. Furder annealed alloys at 400 and 700 °C were prepared in way to determined isothermal sections at chosen temperatures. Existence of the phase were detected with XRD test and composition of detected phases have been determined with EDS test. EDS tests did not detected new compound or even large solubility of third element into intermetalic compouds r solid solution. According to this results it can be concluded that it is not neccessery to introduce new thermodynamic parameters for description of the phase diagrams of the ternary Bi-Ni-Zn system. Based on this conclusion liquidus projectio were predicted and twelve invariant reaction were predicted from which eight are experimentally confirmed by DTA test. Experimentally detected temperatures of invariant reaction are in close agreement with calculated temperatures.

Acknowledgements

This work has been supported by the National Nature Science Foundation of China (project No. 414010049) and the Ministry of Education, Science and Technological Development of the Republic of Serbia (Grant No. OI172037).

Reference

[1] S. Semboshi, S. Sato, A. Iwase, T. Takasugi, Discontinuous precipitates in age-hardening Cu-Ni-Si alloys, Mater. Characterization. 115 (2016) 39-45. https://doi.org/10.1016/j.matchar.2016.03.017

[2] J. Lei, H. Xie, S. Tao, R. Zhang, Z. Lu, Microstructure and Selection of Grain Boundary Phase of Cu-Ni-Si Ternary Alloys, Rare Metal Mat. Eng. 44(12) (2015) 3050-3054. https://doi.org/10.1016/S1875-5372(16)60049-8

[3] C. P. Samal, J. S. Parihar, D. Chaira, The effect of milling and sintering techniq ues on mechanical properties of Cu-graphite metal matrix composite prepared by powder metallurgy route, J. Alloy. Compd. 569 (2013) 95-101. https://doi.org/10.1016/j.jallcom.2013.03.122

[4] R. Masrour, M. Hamedoun, A. Benyoussef, E. K. Hlil, Magnetic properties of mixed Ni-Cu ferrites calculated using mean field approach, J. Magn. Magn. Mater. 363 (2014) 1-5. https://doi.org/10.1016/j.jmmm.2014.03.043

[5] J. Chen, J. Wang, F. Yan, Q. Zhang, Q. Li, Effect of applied potential on the tribocorrosion behaviors of Monel K500 alloy in artificial seawater, Tribol. Int. 81 (2015) 1-8. https://doi.org/10.1016/j.triboint.2014.07.014

[6] W. A. Badawy, M. El-Rabiee, N. H. Helal, H. Nady, The role of Ni in the surface stability of Cu-Al-Ni ternary alloys in sulfatechloride solutions, Electrochim. Acta. 71 (2012) 50-57. https://doi.org/10.1016/j.electacta.2012.03.053
[7] P. Calleja, J. Esteve, P. Cojocaru, L. Magagnin, E. Vallés, E. Gómez, Developing plating baths for the production of reflective Ni-Cu films, Electrochim. Acta. 62 (2012) 381-389. https://doi.org/10.1016/j.electacta.2011.12.049
[8] S. Nagarjuna, M. Srinivas, K. K. Sharma, The grain size dependence of flow stress in a Cu-26Ni-17Zn alloy, Acta Materialia. 48(8) (2000) 1807-1813. https://doi.org/10.1016/S1359-6454(99)00464-4
[9] G. P. Vassilev, K. I. Lilova, J. C. Gachon, Supplementary X-Ray Studies of the Ni-Sn-Bi system, J. Min. Metall. Sect. B-Metall. 43B(2) (2007) 141-150. https://doi.org/10.2298/JMMB0702141V
[10] V. D. Gandova, Ni–Bi–Zn ternary system investigation using diffusion couples technique, J. Min. Metall. Sect. B-Metall. 52B (1) (2016) 113-118. https://doi.org/10.2298/JMMB141101005G
[11] M. Premovic, D. Minic, D. Manasijevic, V. Cosovic, D. Živkovic, I. Derviševic, Experimental investigation and thermodynamic calculations ofthe Bi-In-Ni phase diagram, Thermochim. Acta. 609 (2015) 61–74. http://dx.doi.org/10.1016/j.tca.2015.02.022
[12] D. Minić, M. Premović, N. Tošković, D. Manasijević, V. Ćosović, M. Janaćković, M. Tomović, Experimental investigation and thermodynamic calculations of the Bi-Ni-Pb phase diagram, J. Min. Metall. Sect. B-Metall. 55 (2) B (2019) 157-166. https://doi.org/10.2298/JMMB181128024M
[13] G. P. Vassilev, J. Romanowska, G. Wnuk, Bismuth activity measurements and thermodynamic re-optimization of the Ni–Bi System, Int. J. Mater. Res. 98(6) (2007) 468-475. https://doi.org/10.3139/146.101499
[14] G. Vassilev, V. Gandova, P. Docheva, Comments and reconciliation of the Ni–Bi-system thermodynamic reassessments, Cryst. Res. Technol. 44(1) (2008) 1-6. https://doi.org/ 10.1002/crat.200800391
[15] A. Dinsdale, A. Watson, A. Kroupa, J. Vrestal, A. Zemanova, J. Vizdal: Atlas of Phase Diagrams for the Lead-Free Soldering, COST 531 (Lead-free Soders), Vol. 1, © COST office, 2008, ISBN 978-80-86292-28- 1, Printed in the Czech Republic.
[16] D. V. Malakhov, Thermodynamic assessment of the Bi-Zn system, Calphad. 24 (2000) 1-14. https://doi.org/10.1016/S0364-5916(00)00011-0
[17] K. Xu, S. Liu, Y. Du, L. Dreval, G. Cai, Z. Jin, Thermodynamic investigation of the Mg-Ni-Zn system by experimentsand calculations and its application, J. Alloy. Comp. 784 (2019) 769-787. https://doi.org/10.1016/j.jallcom.2018.12.377
[18] P. Cucka, C. S. Barrett, The crystal structure of Bi and of solid solutions of Pb, Sn, Sb and Te in Bi, Acta Cryst. 15 (1962) 865-872. https://doi.org/10.1107/S0365110X62002297
[19] E. A. Owen, E. L. Yates, X-ray Measurement of the Thermal Expansion of Pure Nickel, Philos. Mag. 7(21) (1936) 809-819. https://doi.org/10.1080/14786443608561628
[20] N. Ridley, Densities of some indium solid solutions, J. Less Common. Met. 8 (1965) 354–357. https://doi.org/10.1016/0022-5088(65)90071-8

[21] E. L. Martinez Pineiro, B. L. Ruiz Herrera, R. Escudero, L. Bucio, Possible coexistence of superconductivity and magnetism in intermetallic NiBi3, Solid State Commun. 151 (2011) 425-429. https://doi.org/10.1016/j.ssc.2011.01.005
[22] M. Ruck, Die Kristallstruktur von BiNi: eine komplexe Ausdünnungsvariante des InNi2-. Typs, Z. Anorg. Allg. Chem. 625 (1999) 2050-2054. https://doi.org/10.1080/14786443608561628
[23] W. Heike, J. Schramm, O. Vaupel, The system nickel-zinc, Metallwirtschaft, Metallwissenschaft, Metalltechnik 15 (1936) 655-662.
[24] R. P. Anantatmula, D. B. Masson, Thermodynamic properties of solid Ni–Zn alloys by atomic absorption, Metall. Trans. 5 (1974) 605–613. https://doi.org/10.1007/BF02644656
[25] A. Johansson, H. Ljung, S. Westman, X-ray and neutron diffraction studies on Γ-Ni,Zn and Γ-Fe,Zn, Acta Chem. Scand. 22 (1968) 2743–2753. https://doi.org/10.3891/*acta.chem.scand.22-2743*
[26] J. K. Critchley, S. Denton, The crystal structure of δ-Ni–Zn, J. Inst. Met. 99 (1971) 26–27.